Optical metamaterial for polarization control

Jiaming Hao (郝加明),[1,2] Qijun Ren (任祺君),[1] Zhenghua An (安正华),[1] Xueqin Huang (黄学勤),[1] Zhanghai Chen (陈张海),[1] Min Qiu (仇旻),[2] and Lei Zhou (周磊)[1,*]

[1]*Surface Physics Laboratory (State Key Laboratory) and Physics Department, Fudan University, Shanghai 200433, China*

[2]*Department of Microelectronics and Applied Physics, Royal Institute of Technology (KTH), Electrum 229, 164 40 Kista, Sweden*

(Received 20 January 2009; published 11 August 2009)

We present the design, characterization, and modeling of a specific optical metamaterial, and employ it to manipulate the light polarizations at optical frequencies. Experimental results reveal that the maximum polarization conversion efficiency, i.e., the energy portion converted from *s* to *p* polarization after reflection, can be as high as 96% at the wavelength of ~685 nm. Simulations and analytical results, which are in reasonable agreements with the experimental results, reveal that the underlying physics are governed by the particular electric and magnetic resonances in the optical metamaterial.

DOI: 10.1103/PhysRevA.80.023807 PACS number(s): 42.25.Ja, 42.25.Bs, 42.25.Lc, 78.20.Bh

Electromagnetic (EM) metamaterials are artificially designed media composed of subwavelength-engineered units, exhibiting unique EM properties that are unattainable with natural materials [1,2]. Recently, metamaterials functioning at optical frequencies gradually appear [3–8]. However, although many fascinating phenomena were theoretically proposed for metamaterials [9–13] and some of them were successfully realized at microwave frequencies [14–16], very few were experimentally confirmed at optical frequencies. This is due to the significantly enhanced challenges faced by both experiment and theory at optical frequencies.

In this paper, we combine experimental and theoretical efforts to demonstrate an important application of optical metamaterials—the polarization control. We present a specifically designed optical metamaterial, and experimentally demonstrate that it can convert light polarization with an efficiency of 96% at $\lambda=685$ nm. Although similar effects had been proven in microwave frequency regime previously [17], realizing such effects at optical frequencies is still highly nontrivial, considering the rareness of metamaterial-based phenomena demonstrated at *optical* frequencies. In addition, the physics considered here is more general, involving both magnetic and electric resonances of the designed optical metamaterial, in contrast to the previous mechanism employing solely magnetic resonances [17].

To illuminate the basic ideas, let us consider the light reflections at an air/metamaterial interface. The reflection coefficients for normally incident lights polarized along *x* and *y* directions are $r_x=(Z_x-1)/(Z_x+1)$, $r_y=(Z_y-1)/(Z_y+1)$, where $Z_x=\sqrt{\mu_y}/\sqrt{\varepsilon_x}$ and $Z_y=\sqrt{\mu_x}/\sqrt{\varepsilon_y}$ are the impedance of the metamaterial for different polarizations. Suppose we shine a light with a polarization $\vec{E}^i=E_0(\hat{x}+\hat{y})$ on the metamaterial, the reflected light would take a polarization $\vec{E}^r=E_0(r_x\hat{x}+r_y\hat{y})$. Then, if the condition $r_x=-r_y$, or equivalently,

$$Z_xZ_y=1 \tag{1}$$

is satisfied, the polarization direction of the reflected light is *perpendicular* to that of the incident one. Condition (1) implies that, to convert light polarizations, the two directions in a metamaterial must satisfy an EM reciprocal principle. Apparently, condition (1) can only be satisfied with a metamaterial since a conventional dielectric (with $\mu=1$) has $Z<1$ for two directions. A limiting solution of Eq. (1) is that $Z_x\rightarrow 0$, $Z_y\rightarrow\infty$, indicating that the system behaves as a perfect electric conductor (PEC) for *x*-polarized light but as a perfect magnetic conductor (PMC) for *y*-polarized light. This is just the situation we realized in microwave frequency regime [17]. At optical frequencies, we cannot achieve a PEC or a PMC but it was recently shown that electric and magnetic resonances could *coexist* in some particular optical metamaterials [18]. In the following, we will design our own metamaterial with *appropriately arranged* EM resonances to make Eq. (1) satisfied at some optical frequencies, and then demonstrate its ability to control light polarizations [19].

As schematically shown in Fig. 1(a), the designed metamaterial consists of a layer of gold rod array and a continuous gold film, separated by a SiO_2 layer. This trilayer structure was fabricated layer by layer with electron-beam evaporation of constituent materials. The 15-nm-thick gold layer was first deposited on a GaAs substrate with 1 nm titanium as the adhesive layer, and then covered by a 60 nm SiO_2 separation layer. The top gold rod array, with a thickness of 15 nm, was fabricated with standard electron-beam lithography and lift-off technique. Each gold rod is sized 240×60 nm^2, and the periodicities of the array are 300 and 150 nm along two directions. A series of samples based on the designs were fabricated with sizes fixed as 100×100 μm^2. Figure 1(b) shows a scanning electron microscopy (SEM) picture of one typical sample.

We performed optical experiments to measure the polarization manipulation effects. The experimental setup is schematically depicted in Fig. 1(c). We used a halogen tungsten lamp as a white light source, which was focused on the sample surface by an objective lens. The reflected light was collected by the same lens and dispersed on the monochromator. Linear polarizers were inserted in the paths of both the incident and reflected lights to control the light polarizations. In our measurements, we set the incident **E** field parallel to a fixed laboratory axis $\hat{x}_0$, and then rotated the sample to change the incident wave polarization with respect to the

*Corresponding author; phzhou@fudan.edu.cn

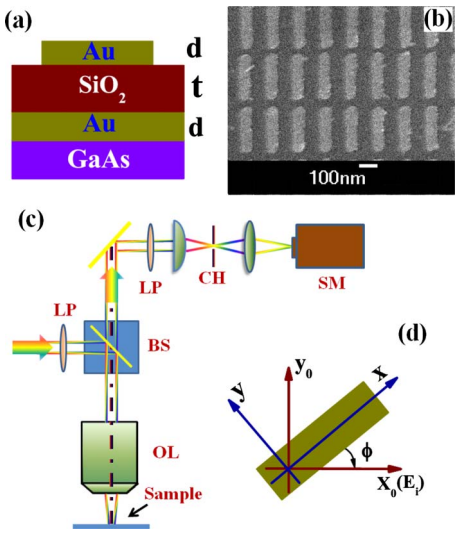

FIG. 1. (Color online) (a) Side-view geometry of the optical metamaterial studied in this paper. (b) Top-view SEM picture of a part of the experimental sample. (c) Scheme of the experimental setup. Here, BS denotes beam splitter, CH confocal hole, LP linear polarizer, OL objective lens, and SM spectrometer. (d) The coordinate system adopted in this paper.

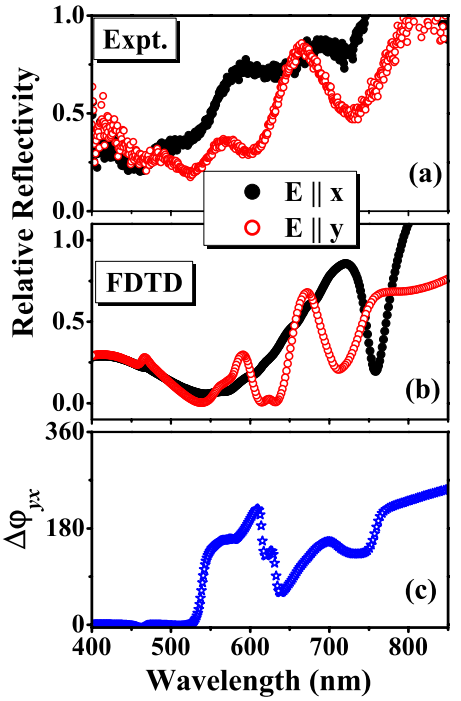

FIG. 2. (Color online) Relative reflectivity as functions of wavelength for normally incident waves with polarizations $\vec{E}\|\hat{x}$ (solid symbols) and $\vec{E}\|\hat{y}$ (open symbols), obtained by (a) measurements and (b) FDTD simulations. (c) Reflection phase difference $\Delta\varphi_{yx}$ as a function of wavelength calculated by the FDTD simulations.

sample [see Fig. 1(d)]. With a fixed incident polarization (assumed as the *s* polarization), we rotated the receiver to measure the reflectance for the reflected signals with the same polarization (denoted as $|r_{ss}|^2$) and that with a *p* polarization (denoted as $|r_{sp}|^2$) [20]. We first rotated the sample so that the incident **E** field is parallel to one of the optical axes, and measured the direct reflection spectra $|r_{ss}|^2$ ($|r_{sp}|^2 \equiv 0$ in this case). The spectra for $\phi=0°$ and $\phi=90°$ cases were depicted in Fig. 2(a) as solid and open symbols, respectively [21]. The spectra clearly show that the designed metamaterial is not totally reflecting since gold is not a perfect metal at optical frequencies. Therefore, previous mechanism for microwave frequencies [17] does not work here.

Now, we rotated the sample such that $\phi=45°$ [see Fig. 1(d)]. Since the incident wave is not polarized along one of the optical axes, both $|r_{ss}|^2$ and $|r_{sp}|^2$ are nonzero, and the measured spectra are shown in Fig. 3(a) as solid and open symbols, respectively [21]. Strong polarization-converted reflection signal ($|r_{sp}|^2$) appear around 680 nm, which is even prominently shown in the polarization conversion ratio (PCR) [defined as $|r_{sp}|^2/(|r_{ss}|^2+|r_{sp}|^2)$] spectra depicted in Fig. 3(b). The maximum PCR value is found as 83% at 680 nm wavelength. We further employed a tunable femtosecond laser as the source to perform the same measurement, and depicted the PCR spectra in Fig. 3(b) as solid stars. The PCR value obtained with laser input is significantly enhanced, and the maximum PCR value is as high as 96% at 685 nm. This is easy to understand since a laser beam has a much better directionality than a focused white light beam.

We performed finite-difference-time-domain (FDTD) simulations [22] to understand these intriguing phenomena. We first calculated the direct reflection spectra for $\phi=0°$ and $\phi=90°$ cases, and depicted the calculated reflectance spectra (denoted as $|r_x|^2$ and $|r_y|^2$) in Fig. 2(b) [21]. Reasonable agreements were found when compared with the experimental spectra, and most experimental features were reproduced [22]. Besides the reflectance, FDTD calculations also provided us the information of reflection phase. From Fig. 2(c) where the calculated reflection phase difference for two polarizations ($\Delta\varphi_{yx}=\varphi_y-\varphi_x$) is shown as a function of wavelength, we find that $\Delta\varphi_{yx}$ approaches 180° within the range of 650–760 nm, coinciding with the frequency range where the PCR peak is found [see Fig. 3(b)]. In fact, by decoupling the incident wave to two independent polarizations, we can calculate the PCR spectra for arbitrary ϕ case (under normal incidence) using the following formula,

$$\mathrm{PCR} = \frac{[|r_x|\sin\phi - |r_y|\cos\phi\cos(\Delta\varphi_{yx})]^2}{[|r_x|\cos\phi + |r_y|\sin\phi\cos(\Delta\varphi_{yx})]^2 + [|r_x|\sin\phi - |r_y|\cos\phi\cos(\Delta\varphi_{yx})]^2}. \quad (2)$$

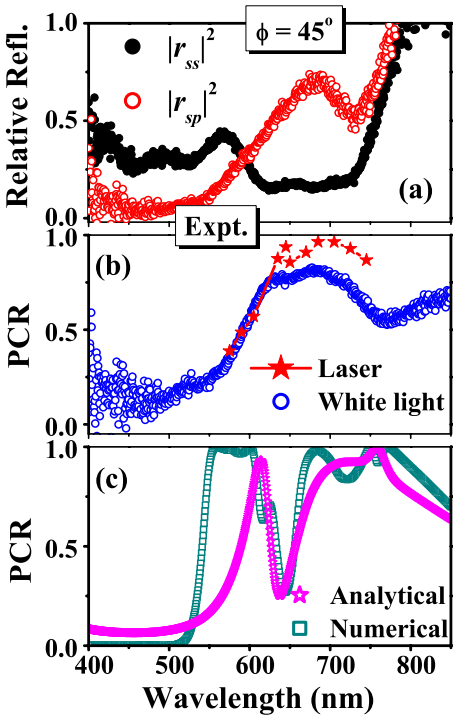

FIG. 3. (Color online) (a) Measured polarization-conserved relative reflectivity ($|r_{ss}|^2$, solid symbols) and polarization-converted relative reflectivity ($|r_{sp}|^2$, open symbols) as functions of wavelength. (b) The calculated PCR as a function of wavelength using the experimental data. (c) The PCR spectra as functions of wavelength obtained by numerical simulations and theoretical analysis.

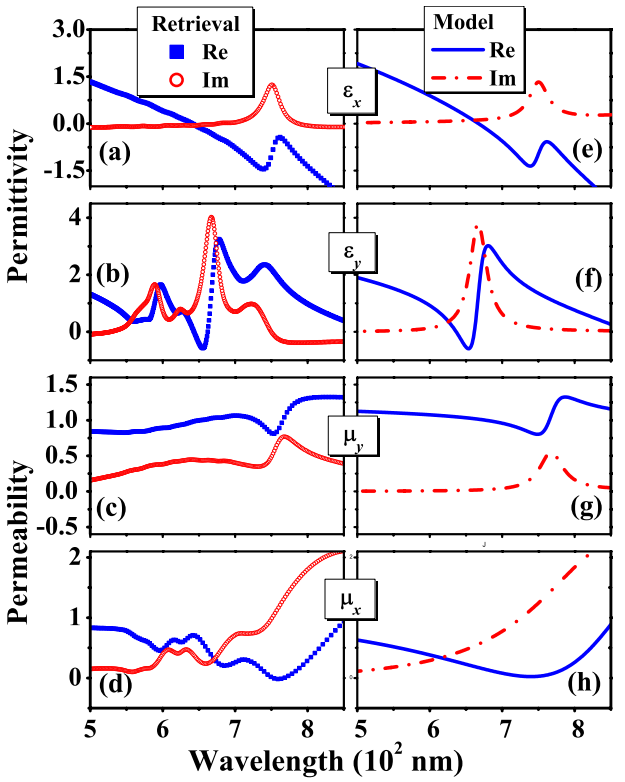

FIG. 4. (Color online) Retrieved effective parameters of the metamaterial, (a) $\tilde{\varepsilon}_x$, (b) $\tilde{\varepsilon}_y$, (c) $\tilde{\mu}_y$, and (d) $\tilde{\mu}_x$, as functions of wavelength; Optical parameters (e) $\tilde{\varepsilon}_x$, (f) $\tilde{\varepsilon}_y$, (g) $\tilde{\mu}_y$, and (h) $\tilde{\mu}_x$ as functions of wavelength, calculated with formulas (3).

The PCR spectra thus calculated is shown in Fig. 3(c) as open squares for ϕ=45°, which is in reasonable agreement with the measured spectra. A straightforward explanation of the large polarization conversion effect is that, around 680 nm wavelength, we have similar reflectance for two linear polarizations (i.e., $|r_x| \approx |r_y|$) but with a nearly 180° reflection phase difference.

We explored the inherent physics behind such unusual phenomena. As we have discussed, optical metamaterial is different from the microwave one since the metal has a finite penetration length here. Therefore, the previously established double-layer effective-medium model [17] is not suitable for the present system. Instead, we find it better to model the present system as a single-layer effective medium with effective permittivity $\tilde{\varepsilon}$ and permeability $\tilde{\mu}$ since the considered wavelength ~700 nm is much larger than the total thickness of the structure of 90 nm. We have retrieved the effective optical parameters using the FDTD simulated transmission/reflection coefficients [3,23], and plotted in Figs. 4(a)–4(d) the retrieved values of $\tilde{\varepsilon}_x$, $\tilde{\varepsilon}_y$, $\tilde{\mu}_x$, and $\tilde{\mu}_y$ [24]. The retrieved parameters can be well described by the following Lorentz models,

$$\varepsilon_x = 4 - \frac{656^2}{f^2 + i \times 2 \times f} + \frac{520^2}{205^2 - f^2 - i \times 17.5 \times f} + \frac{90^2}{400^2 - f^2 - i \times 17 \times f},$$

$$\varepsilon_y = 3.3 - \frac{655^2}{f^2 + i \times 2 \times f} + \frac{180^2}{450^2 - f^2 - i \times 19 \times f},$$

$$\mu_x = 1 + \frac{310^2}{350^2 - f^2 - i \times 130 \times f},$$

$$\mu_y = 1.1 + \frac{135^2}{160^2 - f^2 - i \times 25 \times f} + \frac{65^2}{391^2 - f^2 - i \times 17 \times f}, \quad (3)$$

as shown in Figs. 4(e)–4(h). Here f denotes the frequency in THz. It is interesting to note that, beside the common Drude-like contributions in ε_x and ε_y, which originate from the material itself, formulas (3) imply that a series of additional EM resonances exist in such a metamaterial. The magnetic resonances are induced by an antisymmetric coupling of the currents flowing in the two metallic layers, which are similar to those found at microwave frequencies [17]. For the electric resonances, the electric current in each gold rod is *parallel* to that flowing in the continuous gold film, forming a symmetric mode [18]. In general, these EM resonances occur at different wavelengths dictated by the geometry. Thus, our system is an ideal anisotropic optical material possessing wide parameter tunability so that it can fulfill many applications with appropriate designs. We have calculated the PCR spectrum employing the generalized 4×4 transfer-matrix method [25] with effective parameters given by Eq. (3), and

found that the results [depicted in Fig. 3(c) as open stars] are in reasonable agreements with both the direct numerical results and the experimental data.

The analytical model helps us to understand the physics more clearly. Since both electric and magnetic resonances exist in our system, we carefully designed the optical metamaterial to make condition (1) satisfied at some particular frequencies. Indeed, we plotted the real and imaginary parts of Z_xZ_y as functions of wavelength in Fig. 5(b), compared with the PCR spectra replotted in Fig. 5(a). As expected, we do find that $Z_xZ_y \approx 1$ at two wavelengths 628 and 766 nm, which directly explains the two PCR peaks observed both experimentally and theoretically in Figs. 5(a), 3(b), and 3(c). We note that condition (1), obtained based on a single air/metamaterial interface, is not *rigorously* applicable to the present slab case. Nevertheless, we find that condition (1) is intuitive to help understand the inherent physics, and is helpful for future designs of similar systems.

In summary, we designed and fabricated optical metamaterials to manipulate light polarizations at visible frequencies. Experiments reveal that the maximum PCR value reaches 96% at 685 nm, and the underlying physics are governed by appropriately designed EM resonances. Our system can find many applications in practice. Since the proposed scheme is operated on a reflection geometry, it could be a good substitute when usual optical wave plates (designed for a transmission geometry) are inconvenient to apply. In addition, compared with the high-reflective multilayer mirrors commonly employed to control the polarization of reflected light [26], our system is much thinner than the operation wavelength, and thus is useful in miniaturized environments.

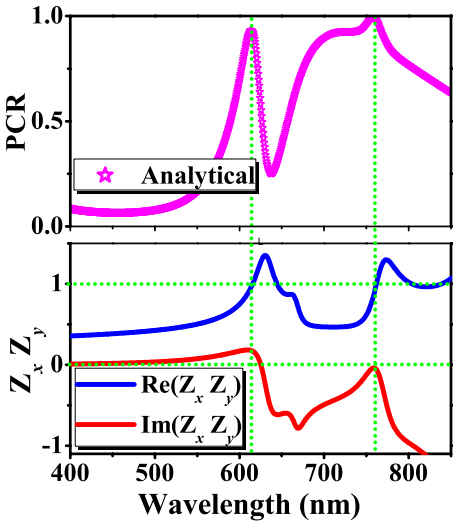

FIG. 5. (Color online) (a) The PCR spectrum as a function of wavelength obtained by theoretical analysis. (b) Real and imaginary parts of Z_xZ_y as functions of wavelength.

This work was supported by the China-973 Programs (Contracts No. 2004CB719803 and No. 2006CB921506), the NSFC (Contracts No. 60725417, No. 10744007, and No. 10804019), PCSIRT, Shanghai Science and Technology Committee (Contract No. 08dj1400302), JST, the Swedish Foundation for Strategic Research (SSF), and the Swedish Research Council (VR). We thank Professor S. Komiyama at University of Tokyo for providing sample fabrication facilities.

[1] D. R. Smith, W. J. Padilla, D. C. Vier, S. C. Nemat-Nasser, and S. Schultz, Phys. Rev. Lett. **84**, 4184 (2000).
[2] D. R. Smith, J. B. Pendry, and M. C. K. Wiltshire, Science **305**, 788 (2004).
[3] S. Zhang, W. Fan, N. C. Panoiu, K. J. Malloy, R. M. Osgood, and S. R. J. Brueck, Phys. Rev. Lett. **95**, 137404 (2005).
[4] V. M. Shalaev, W. S. Cai, U. K. Chettiar, Hsiao-Kuan Yuan, A. K. Sarychev, V. P. Drachev, and A. V. Kildishev, Opt. Lett. **30**, 3356 (2005).
[5] G. Dolling, C. Enkrich, M. Wegener, C. M. Soukoulis, and S. Linden, Opt. Lett. **31**, 1800 (2006).
[6] S. Zhang, W. J. Fan, K. J. Malloy, S. R. J. Brueck, N. C. Panoiu, and R. M. Osgood, J. Opt. Soc. Am. B **23**, 434 (2006).
[7] G. Dolling, M. Wegener, C. M. Soukoulis, and S. Linden, Opt. Lett. **32**, 53 (2007).
[8] V. M. Shalaev, Nat. Photonics **1**, 41 (2007).
[9] N. Engheta, Science **317**, 1698 (2007).
[10] A. Alù and N. Engheta, Nat. Photonics **2**, 307 (2008).
[11] J. B. Pendry, Phys. Rev. Lett. **85**, 3966 (2000).
[12] U. Leonhardt, Science **312**, 1777 (2006).
[13] J. B. Pendry, D. Schurig, and D. R. Smith, Science **312**, 1780 (2006).
[14] R. A. Shelby, D. R. Smith, and S. Schutlz, Science **292**, 77 (2001).
[15] H. Q. Li, J. M. Hao, L. Zhou, Z. Y. Wei, L. K. Gong, H. Chen, and C. T. Chan, Appl. Phys. Lett. **89**, 104101 (2006).
[16] D. Schurig, J. J. Mock, B. J. Justice, S. A. Cummer, J. B. Pendry, A. F. Starr, and D. R. Smith, Science **314**, 977 (2006).
[17] J. Hao, Y. Yuan, L. Ran, T. Jiang, J. A. Kong, C. T. Chan, and L. Zhou, Phys. Rev. Lett. **99**, 063908 (2007).
[18] V. A. Podolskiy, A. K. Sarychev, and V. M. Shalaev, J. Nonlinear Opt. Phys. Mater. **11**, 65 (2002); Uday K. Chettiar, A. V. Kildishev, T. A. Klar, and V. M. Shalaev, Opt. Express **14**, 7872 (2006).
[19] Those studies in [18] mainly focused on the situations where the polarization is conserved after reflection and did not discuss the effect of polarization control.
[20] We found that the transmissions through the beam splitter are polarization sensitive. In the wavelength range of 450–800 nm, the bare transmittance of *p*-polarized light is roughly 45.2% that of the *s*-polarized light. Therefore, we multiply the raw data $|r_{sp}|^2$ by a factor 2.21 to account for such an effect.
[21] Both experimental data and simulation results are referenced by the reflection spectrum measured or calculated with a semi-infinite Si slab. As $\lambda > 750$ nm, the relative reflectivity is higher than one since our system possesses a higher reflectivity than a Si slab.
[22] CONCERTO 7.0, Vector Fields Limited, England (2008). In

our simulations, we took the permittivity of gold as $\varepsilon=9.0-(1.37\times10^{16})^2/[\omega^2+i(1.0027\times10^{14})\omega]$, the refractive index of SiO_2 as 1.5, and the permittivity of the semi-infinite GaAs substrate as 10.8. The discrepancies between FDTD and experimental results are inevitable since there are imperfections in the sample [see Fig. 1(b)], which do not exist in FDTD simulations; the incident wave is a focused Gaussian beam in experiments but is an ideal plane wave in FDTD simulations; moreover also the Drude model of gold's permittivity becomes inaccurate at wavelength $\lambda<550$ nm.

[23] D. R. Smith, S. Schultz, P. Markos, and C. M. Soukoulis, Phys. Rev. B **65**, 195104 (2002).

[24] The retrieved parameters might be less reliable in the wavelength regime $\lambda<2a\approx600$ nm where high-order diffractions appear. However, the essential physical behaviors should not change. Also, in the most interesting wavelength range around 685 nm, our retrieval calculations are reliable. In fact, other groups also employed the retrieval method to determine the effective parameters near the condition $\lambda\approx2a$, see, for example, [7]; H.-K. Yuan, U. K. Chettiar, W. S. Cai, A. V. Kildishev, A. Boltasseva, V. P. Drachev, and V. M. Shalaev, Opt. Express **15**, 1076 (2007).

[25] J. M. Hao and Lei Zhou, Phys. Rev. B **77**, 094201 (2008).

[26] M. F. Weber, C. A. Stover, L. R. Gilbert, T. J. Nevitt, and A. J. Ouderkirk, Science **287**, 2451 (2000).